



**Measurement of the $\gamma\gamma \rightarrow \pi^+\pi^-$ and
 $\gamma\gamma \rightarrow K^+K^-$ processes
at energies of 2.4–4.1 GeV**

Belle Collaboration

H. Nakazawa^j, S. Uehara^j, K. Abe^j, K. Abe^{at}, H. Aihara^{av},
M. Akatsu^x, Y. Asano^{bb}, V. Aulchenko^b, T. Aushevⁿ,
S. Bahinipati^f, A. M. Bakich^{aq}, Y. Ban^{aj}, S. Banerjee^{ar},
I. Bedny^b, U. Bitenc^o, I. Bizjak^o, S. Blyth^{ac}, A. Bondar^b,
A. Bozek^{ad}, M. Bračko^{j,v,o}, J. Brodzicka^{ad}, A. Chen^z,
B. G. Cheon^d, R. Chistovⁿ, Y. Choi^{ap}, Y. K. Choi^{ap},
A. Chuvikov^{ak}, J. Dalseno^w, M. Danilovⁿ, M. Dash^{bd},
A. Drutskoy^f, S. Eidelman^b, Y. Enari^x, D. Epifanov^b,
S. Fratina^o, N. Gabyshev^b, A. Garmash^{ak}, T. Gershon^j,
G. Gokhroo^{ar}, K. Hayasaka^x, H. Hayashii^y, Y. Hoshi^{at},
S. Hou^z, W.-S. Hou^{ac}, T. Iijima^x, A. Imoto^y, K. Inami^x,
A. Ishikawa^j, R. Itoh^j, M. Iwasaki^{av}, Y. Iwasaki^j,
J. H. Kang^{be}, J. S. Kang^q, S. U. Kataoka^y, N. Katayama^j,
H. Kawai^c, T. Kawasaki^{af}, H. R. Khan^{aw}, H. Kichimi^j,
H. J. Kim^s, J. H. Kim^{ap}, S. K. Kim^{ao}, S. M. Kim^{ap},
S. Korpar^{v,o}, P. Križan^{u,o}, P. Krokovny^b, R. Kulasiri^f,
C. C. Kuo^z, A. Kuzmin^b, Y.-J. Kwon^{be}, G. Leder^m,
S. E. Lee^{ao}, T. Lesiak^{ad}, J. Li^{an}, S.-W. Lin^{ac}, D. Liventsevⁿ,
G. Majumder^{ar}, F. Mandl^m, T. Matsumoto^{ay}, A. Matyja^{ad},
W. Mitaroff^m, H. Miyake^{ah}, H. Miyata^{af}, R. Mizukⁿ,
D. Mohapatra^{bd}, T. Mori^{aw}, T. Nagamine^{au}, Y. Nagasaka^k,
E. Nakano^{ag}, M. Nakao^j, Z. Natkaniec^{ad}, S. Nishida^j,
O. Nitoh^{az}, T. Nozaki^j, S. Ogawa^{as}, T. Ohshima^x, T. Okabe^x,
S. Okuno^p, S. L. Olsenⁱ, W. Ostrowicz^{ad}, P. Pakhlovⁿ,

H. Palka^{ad}, C. W. Park^{ap}, H. Park^s, N. Parslow^{aq},
L. S. Peak^{aq}, R. Pestotnik^o, L. E. Pilonen^{bd}, H. Sagawa^j,
Y. Sakai^j, N. Sato^x, T. Schietinger^t, O. Schneider^t,
J. Schümann^{ac}, K. Senyo^x, H. Shibuya^{as}, B. Schwartz^b,
J. B. Singh^{ai}, A. Somov^f, N. Soni^{ai}, R. Stamen^j, S. Stanič^{bb,1},
M. Starič^o, K. Sumisawa^{ah}, T. Sumiyoshi^{ay}, S. Y. Suzuki^j,
O. Tajima^j, F. Takasaki^j, N. Tamura^{af}, M. Tanaka^j,
Y. Teramoto^{ag}, X. C. Tian^{aj}, T. Tsuboyama^j, T. Tsukamoto^j,
T. Uglovⁿ, S. Uno^j, G. Varnerⁱ, S. Villa^t, C. C. Wang^{ac},
C. H. Wang^{ab}, M. Watanabe^{af}, Y. Watanabe^{aw},
B. D. Yabsley^{bd}, A. Yamaguchi^{au}, Y. Yamashita^{ae},
M. Yamauchi^j, J. Ying^{aj}, Y. Yusa^{au}, L. M. Zhang^{an},
Z. P. Zhang^{an}, V. Zhilich^b, and D. Žontar^{u,o}

^a*Aomori University, Aomori, Japan*

^b*Budker Institute of Nuclear Physics, Novosibirsk, Russia*

^c*Chiba University, Chiba, Japan*

^d*Chonnam National University, Kwangju, Republic of Korea*

^e*Chuo University, Tokyo, Japan*

^f*University of Cincinnati, Cincinnati, OH, USA*

^g*University of Frankfurt, Frankfurt, Germany*

^h*Gyeongsang National University, Chinju, Republic of Korea*

ⁱ*University of Hawaii, Honolulu, HI, USA*

^j*High Energy Accelerator Research Organization (KEK), Tsukuba, Japan*

^k*Hiroshima Institute of Technology, Hiroshima, Japan*

^l*Institute of High Energy Physics, Chinese Academy of Sciences, Beijing, PR
China*

^m*Institute of High Energy Physics, Vienna, Austria*

ⁿ*Institute for Theoretical and Experimental Physics, Moscow, Russia*

^o*J. Stefan Institute, Ljubljana, Slovenia*

^p*Kanagawa University, Yokohama, Japan*

^q*Korea University, Seoul, Republic of Korea*

^r*Kyoto University, Kyoto, Japan*

^s*Kyungpook National University, Taegu, Republic of Korea*

^t*Swiss Federal Institute of Technology of Lausanne, EPFL, Lausanne, Switzerland*

^u*University of Ljubljana, Ljubljana, Slovenia*

^v*University of Maribor, Maribor, Slovenia*

- ^w *University of Melbourne, Victoria, Australia*
- ^x *Nagoya University, Nagoya, Japan*
- ^y *Nara Women's University, Nara, Japan*
- ^z *National Central University, Chung-li, Taiwan*
- ^{aa} *National Kaohsiung Normal University, Kaohsiung, Taiwan*
- ^{ab} *National United University, Miao Li, Taiwan*
- ^{ac} *Department of Physics, National Taiwan University, Taipei, Taiwan*
- ^{ad} *H. Niewodniczanski Institute of Nuclear Physics, Krakow, Poland*
- ^{ae} *Nihon Dental College, Niigata, Japan*
- ^{af} *Niigata University, Niigata, Japan*
- ^{ag} *Osaka City University, Osaka, Japan*
- ^{ah} *Osaka University, Osaka, Japan*
- ^{ai} *Panjab University, Chandigarh, India*
- ^{aj} *Peking University, Beijing, PR China*
- ^{ak} *Princeton University, Princeton, NJ, USA*
- ^{al} *RIKEN BNL Research Center, Brookhaven, NY, USA*
- ^{am} *Saga University, Saga, Japan*
- ^{an} *University of Science and Technology of China, Hefei, PR China*
- ^{ao} *Seoul National University, Seoul, Republic of Korea*
- ^{ap} *Sungkyunkwan University, Suwon, Republic of Korea*
- ^{aq} *University of Sydney, Sydney, NSW, Australia*
- ^{ar} *Tata Institute of Fundamental Research, Bombay, India*
- ^{as} *Toho University, Funabashi, Japan*
- ^{at} *Tohoku Gakuin University, Tagajo, Japan*
- ^{au} *Tohoku University, Sendai, Japan*
- ^{av} *Department of Physics, University of Tokyo, Tokyo, Japan*
- ^{aw} *Tokyo Institute of Technology, Tokyo, Japan*
- ^{ay} *Tokyo Metropolitan University, Tokyo, Japan*
- ^{az} *Tokyo University of Agriculture and Technology, Tokyo, Japan*
- ^{ba} *Toyama National College of Maritime Technology, Toyama, Japan*
- ^{bb} *University of Tsukuba, Tsukuba, Japan*
- ^{bc} *Utkal University, Bhubaneswer, India*
- ^{bd} *Virginia Polytechnic Institute and State University, Blacksburg, VA, USA*
- ^{be} *Yonsei University, Seoul, Republic of Korea*

Abstract

We have measured $\pi^+\pi^-$ and K^+K^- production in two-photon collisions using 87.7fb^{-1} of data collected with the Belle detector at the asymmetric energy e^+e^- collider KEKB. The cross sections are measured to high precision in the two-photon center-of-mass energy (W) range between $2.4\text{GeV} < W < 4.1\text{GeV}$ and angular region $|\cos\theta^*| < 0.6$. The cross section ratio $\sigma(\gamma\gamma \rightarrow K^+K^-)/\sigma(\gamma\gamma \rightarrow \pi^+\pi^-)$ is measured to be $0.89 \pm 0.04(\text{stat.}) \pm 0.15(\text{syst.})$ in the range of $3.0\text{GeV} < W < 4.1\text{GeV}$, where the ratio is energy independent. We observe a $\sin^{-4}\theta^*$ behavior of the cross section in the same W range. Production of χ_{c0} and χ_{c2} mesons is observed in both $\gamma\gamma \rightarrow \pi^+\pi^-$ and $\gamma\gamma \rightarrow K^+K^-$ modes.

Key words: two-photon collisions, mesons, QCD, charmonium

PACS: 12.38Qk, 13.25.Gv, 13.66.Bc, 13.85.Lg

1 Introduction

Exclusive processes with hadronic final states test various model calculations motivated by perturbative or non-perturbative QCD. Two-photon production of exclusive hadronic final states is particularly attractive due to the absence of strong interactions in the initial state and the possibility of calculating $\gamma\gamma \rightarrow q\bar{q}$ amplitudes. The perturbative QCD calculation by Brodsky and Lepage (BL) [1] is based on factorization of the amplitude into a hard scattering amplitude for $\gamma\gamma \rightarrow q\bar{q}q\bar{q}$ and a single-meson distribution amplitude. Their prediction gives the dependence on the center-of-mass (c.m.) energy $W(\equiv\sqrt{s})$ and scattering angle θ^* for $\gamma\gamma \rightarrow M^+M^-$ processes

$$\frac{d\sigma}{d|\cos\theta^*|}(\gamma\gamma \rightarrow M^+M^-) \approx \frac{16\pi\alpha^2}{s} \frac{|F_M(s)|^2}{\sin^4\theta^*}, \quad (1)$$

where M represents a meson and F_M denotes its electromagnetic form factor. Vogt [2], based on the perturbative approach, claimed a need for soft contributions, as his result for the hard contribution was well below the experimental cross section obtained by CLEO [3].

Diehl, Kroll and Vogt (DKV) proposed [4] the soft handbag contribution to two-photon annihilation into pion or kaon pairs at large energy and momentum transfers, in which the amplitude is expressed by a hard $\gamma\gamma \rightarrow q\bar{q}$ subprocess and a form factor describing the soft transition from $q\bar{q}$ to the meson pair.

¹ on leave from Nova Gorica Polytechnic, Nova Gorica, Slovenia

DKV, as well as BL, predict the $\sin^{-4}\theta^*$ dependence of the angular differential cross section, which is an important test of these approaches. It is interesting to investigate experimentally an energy scale where those theoretical predictions become valid. The recent measurements of $\gamma\gamma \rightarrow \pi^+\pi^-$ and K^+K^- performed by ALEPH [5] are consistent, within their errors, with the BL's prediction of the energy dependence, but not the normalization. However, their dataset is not sufficient to conclusively test the W and $\sin^{-4}\theta^*$ dependences.

In this report, we measure $\gamma\gamma \rightarrow \pi^+\pi^-$ and $\gamma\gamma \rightarrow K^+K^-$ processes with high precision, and make quantitative comparisons with QCD predictions. This analysis is based on an 87.7fb^{-1} data sample collected at or near the $\Upsilon(4S)$ resonance energy, accumulated with the Belle detector [6] located at KEKB [7].

2 KEKB accelerator and Belle detector

KEKB is a colliding beam accelerator of 8 GeV electrons and 3.5 GeV positrons designed to produce copious $B\bar{B}$ meson pairs to observe CP violation.

The Belle detector, with a 1.5 T solenoidal magnetic field, surrounds the interaction point and subtends the polar angle range $17^\circ < \theta_{\text{lab}} < 150^\circ$, measured from the z axis, which is aligned opposite the positron beam. It is described in detail in Ref. [6]. Briefly, charged track momenta and their decay points are measured by the central drift chamber (CDC) and silicon vertex detector (SVD). The hadron identity of these charged tracks is determined using information from the time-of-flight counters (TOF), the aerogel threshold Čerenkov counters (ACC), and the specific ionization in the CDC. Hadron/electron discrimination is performed using the above information as well as the energy deposition and shower profile in the segmented CsI(Tl)-crystal electromagnetic calorimeter (ECL). Hadron/muon discrimination is achieved using information from the neutral-kaon and muon detector (KLM), which consists of glass resistive plate counters embedded in the solenoid's iron flux return.

3 Event selection

The signal events are collected predominantly by a trigger that requires two charged tracks penetrating through the CDC and TOF, with an opening angle in the $r\varphi$ plane (perpendicular to the z axis) of at least 135° .

We select signal candidates according to the following criteria. There must be exactly two oppositely-charged reconstructed tracks satisfying the following

conditions: $-0.47 \leq \cos \theta_{\text{lab}} \leq 0.82$ for the polar angle θ_{lab} of each track; $p_t > 0.8$ GeV/ c for the momentum component in the $r\varphi$ plane of each track; $dr \leq 1$ cm and $|dz| < 2$ cm for the origin of each track relative to the nominal e^+e^- collision point; and $|dz_1 - dz_2| \leq 1$ cm for the two tracks' origin difference along the z axis, where the origin is defined by the closest approach of the track to the nominal collision point in the $r\varphi$ plane. The event is vetoed if it contains any other reconstructed charged track with transverse momentum above 0.1 GeV/ c .

Cosmic rays are suppressed by demanding that the opening angle α between the two tracks satisfy $\cos\alpha \geq -0.997$. The signal is enriched relative to other backgrounds by requiring that the scalar sum of the momentum of the two tracks be below 6 GeV/ c , the total energy deposited in the ECL be below 6 GeV, the magnitude of the net transverse momentum of the above-selected two charged tracks in the e^+e^- c.m. frame be below 0.2 GeV/ c (this condition is tightened in the next section), the invariant mass of these two tracks be below 4.5 GeV/ c^2 , and that the squared missing mass of the event be above 2 GeV²/ c^4 . Here, the two tracks are assumed to be massless particles. The latter two requirements eliminate radiative Bhabha and initial state radiation events. The remaining events consist of two-photon production of e^+e^- , $\mu^+\mu^-$, $\pi^+\pi^-$, K^+K^- , and $p\bar{p}$ final states as well as unvetted $e^+e^- \rightarrow \tau^+\tau^-$ events according to a Monte Carlo (MC) study [8].

The predicted versus measured range and transverse deviation of hits in the KLM are used to construct a normalized likelihood \mathcal{R}_μ that a track extrapolated from the CDC is a muon rather than a pion or kaon. Here, we classify an event as arising from $\gamma\gamma \rightarrow \mu^+\mu^-$ if either track has $\mathcal{R}_\mu > 0.66$. Similarly, the TOF, ACC, CDC, and ECL information is used to construct a normalized likelihood \mathcal{R}_e that a reconstructed track is an electron rather than a hadron. We classify an event as arising from $\gamma\gamma \rightarrow e^+e^-$ if either track has $\mathcal{R}_e > 0.66$. For above two separations 93% of signal events survive for both modes according to the MC study described later. The TOF, ACC and CDC information is used to construct another normalized likelihood \mathcal{R}_p that a reconstructed track is a proton rather than a kaon, with a high value corresponding to a proton-like track. The scatterplot of this quantity for the negative track *vs.* that for the positive track in each event is shown in Fig. 1(a). Note that the peak near the origin contains both K^+K^- and $\pi^+\pi^-$ candidates. Events above the hyperbolic curve $(\mathcal{R}_p^- - 1.01)(\mathcal{R}_p^+ - 1.01) = 0.0101$, shown in the inset of Fig. 1(a), are deemed to arise from $\gamma\gamma \rightarrow p\bar{p}$.

After removing events that appear to arise from two-photon production of $\mu^+\mu^-$, e^+e^- , and $p\bar{p}$ according to the above criteria, the remaining sample consists of two-photon production of K^+K^- , $\pi^+\pi^-$, and residual $\mu^+\mu^-$, as well as $e^+e^- \rightarrow \tau^+\tau^-$ production where each τ lepton decays to a single pion or muon. Information from the TOF, ACC, and CDC is used to form a normalized

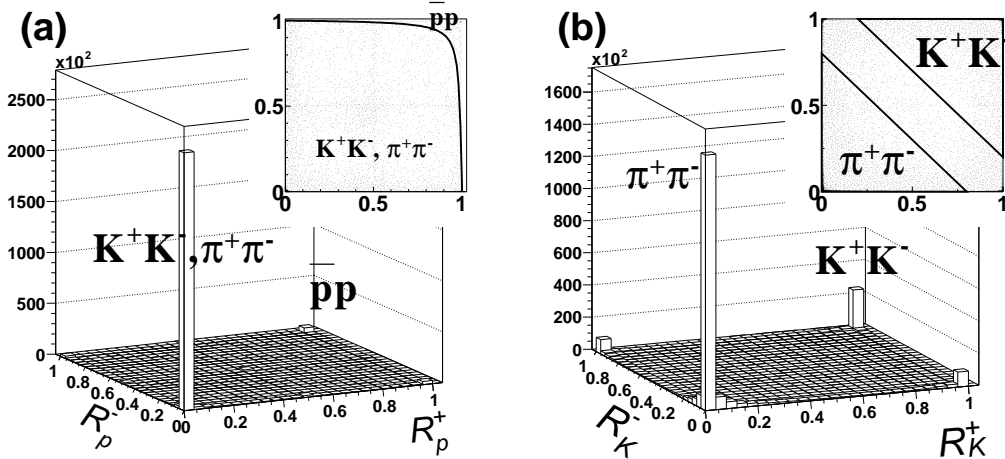


Fig. 1. Two-dimensional plots of likelihood ratios for hadron identification: (a) \mathcal{R}_p and (b) \mathcal{R}_K . The cut boundaries are shown in the top-view insets.

likelihood ratio \mathcal{R}_K that a reconstructed track is a kaon rather than a pion (or muon), with a high value corresponding to a kaon-like track. The scatter plot of this quantity for the negative track *vs.* that for the positive track is shown in Fig. 1(b). Note that the peak near the origin contains $\pi^+\pi^-$, $\tau^+\tau^-$, and residual $\mu^+\mu^-$ events. Events above the diagonal line $\mathcal{R}_K^- + \mathcal{R}_K^+ = 1.2$, shown in the inset of Fig. 1(b), are classified as K^+K^- candidates, while events below the line $\mathcal{R}_K^- + \mathcal{R}_K^+ = 0.8$ are classified as $\pi^+\pi^-$ candidates (including $\tau^+\tau^-$ and residual $\mu^+\mu^-$ backgrounds). Events in the diagonal band between these two lines are discarded.

The $\pi^+\pi^-$ sample is somewhat contaminated by non-exclusive two-photon background $\gamma\gamma \rightarrow \pi^+\pi^-X$ as well as the $e^+e^- \rightarrow \tau^+\tau^-$ process, in roughly equal proportion. We note that these backgrounds appear at high values of the magnitude of the net transverse momentum $|\mathbf{p}_t^+ + \mathbf{p}_t^-|$ in the e^+e^- c.m. frame, and are often accompanied by photons from the prompt decay of a neutral pion in the final state. Therefore, we reject events in the $\pi^+\pi^-$ sample that contain a photon with energy above 400 MeV (E_γ -veto). The distributions of $|\mathbf{p}_t^+ + \mathbf{p}_t^-|$ for the $\pi^+\pi^-$ candidates before and after application of this veto are shown as the histograms in Fig. 2(a).

The yields of the $\pi^+\pi^-$ and K^+K^- events are expressed as functions of three variables: W derived from the invariant mass of the two mesons, $|\cos\theta^*|$ and $|\mathbf{p}_t^+ + \mathbf{p}_t^-|$. Eighty-five 20 MeV wide bins in W times six bins in the cosine of the $\gamma\gamma$ c.m. scattering angle θ^* times twenty bins in net transverse momentum are used in the ranges $2.4 \text{ GeV} < W < 4.1 \text{ GeV}$, $|\cos\theta^*| < 0.6$, and $|\mathbf{p}_t^+ + \mathbf{p}_t^-| < 0.2 \text{ GeV}/c$.

4 Background rejection

The spectrum of the residual $\gamma\gamma \rightarrow \mu^+\mu^-$ background within the $\pi^+\pi^-$ sample is obtained from a MC simulation, based on a full $\mathcal{O}(\alpha^4)$ QED calculation [9], with a data sample corresponding to an integrated luminosity of 174.2 fb^{-1} that is processed by the full detector simulation program and then subjected to trigger simulation and the above event selection criteria. After calibration of the muon identification efficiency to match that in the data using identified $\gamma\gamma \rightarrow \mu^+\mu^-$ events, the residual $\mu^+\mu^-$ background is scaled by the integrated luminosity ratio and then subtracted.

The excess in the E_γ -vetoed histogram of Fig. 2(a) above the smooth curve from the signal MC—described in more detail below—is attributed to non-exclusive $\gamma\gamma \rightarrow \pi^+\pi^-X$ events that are not rejected by the E_γ -veto; most of the $e^+e^- \rightarrow \tau^+\tau^-$ events are rejected by this veto. A similar excess appears in Fig. 2(b) for the $\gamma\gamma \rightarrow K^+K^-$ process. Assuming that this remaining background is proportional to net transverse momentum, we determine the slope using the difference between data and MC in the range $0 < |\mathbf{p}_t^+ + \mathbf{p}_t^-| < 0.17 \text{ GeV}/c$ for each 200 MeV wide W bin, then smooth the so-determined slopes by fitting them to a cubic polynomial in W . We verify that there is no dependence on the scattering angle θ^* . Using the smoothed slope, the estimated non-exclusive background is subtracted from each bin. Finally, we restrict our signal region to net transverse momentum below 0.05 (0.10) GeV/ c for $\gamma\gamma \rightarrow \pi^+\pi^-$ ($\gamma\gamma \rightarrow K^+K^-$). The background-subtracted yields, integrated over net transverse momentum and scattering angle, are shown as a function of W in Fig. 3.

The signatures of the $\chi_{c0}(1P)$ and $\chi_{c2}(1P)$ resonances are observed in both $\pi^+\pi^-$ and K^+K^- channels. By fitting each W distribution outside the range 3.3–3.7 GeV to a cubic polynomial, we see an excess of 129 (153) events in the $\pi^+\pi^-$ (K^+K^-) channel in the χ_{c0} range of 3.34–3.44 GeV and a corresponding excess of 54 (33) events in the χ_{c2} range of 3.54–3.58 GeV. We obtain consistent results from a fit of each distribution to a cubic polynomial plus a Breit-Wigner (χ_{c0}) or a Gaussian (χ_{c2}) peak. Assuming a flat ($\sin^4\theta^*$) shape for the χ_{c0} (χ_{c2}) resonance [10], we subtract the above excesses bin by bin from each angular distribution in the above W ranges. The χ_{c0} statistical significance is 6.2σ (8.2σ) in the $\pi^+\pi^-$ (K^+K^-) channel, where σ is the standard deviation. The χ_{c2} statistical significance is 4.8σ (3.7σ) in the $\pi^+\pi^-$ (K^+K^-) channel. The significances are taken from the square root of the difference of the goodness-of-fit values from the two fits where the peak term in the above fit function is included or excluded.

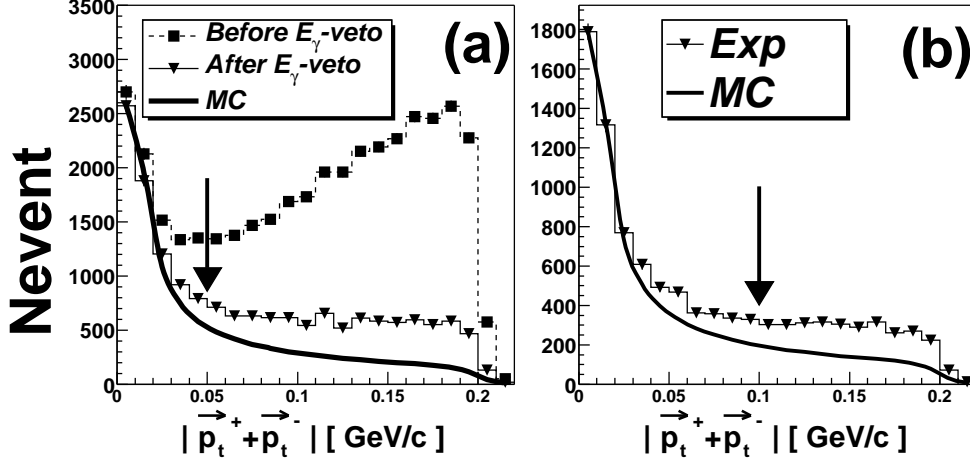


Fig. 2. $|\mathbf{p}_t^+ + \mathbf{p}_t^-|$ distribution for $\pi^+\pi^-$ (a) and K^+K^- (b) candidates. The dashed and solid histograms in $\pi^+\pi^-$ indicate the distribution of events before and after E_γ -veto (which is not applied to the K^+K^- candidates), respectively. The arrows indicate the upper boundaries of $|\mathbf{p}_t^+ + \mathbf{p}_t^-|$ for the signal. The residual muon background has been subtracted from the $\pi^+\pi^-$ distribution. The curves show the signal MC distribution which is normalized to the signal candidates at the leftmost bin.

5 Derivation of the cross section

The differential cross section for a two-photon process to a two-body final state arising from an electron-positron collision is given by

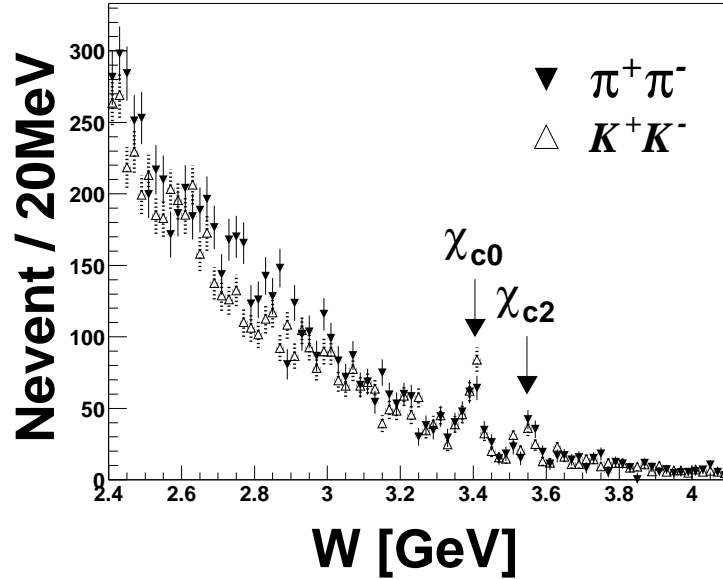


Fig. 3. Number of events ($|\cos \theta^*| < 0.6$) obtained for the $\gamma\gamma \rightarrow \pi^+\pi^-$ (solid) and $\gamma\gamma \rightarrow K^+K^-$ (dashed) samples after the background subtraction.

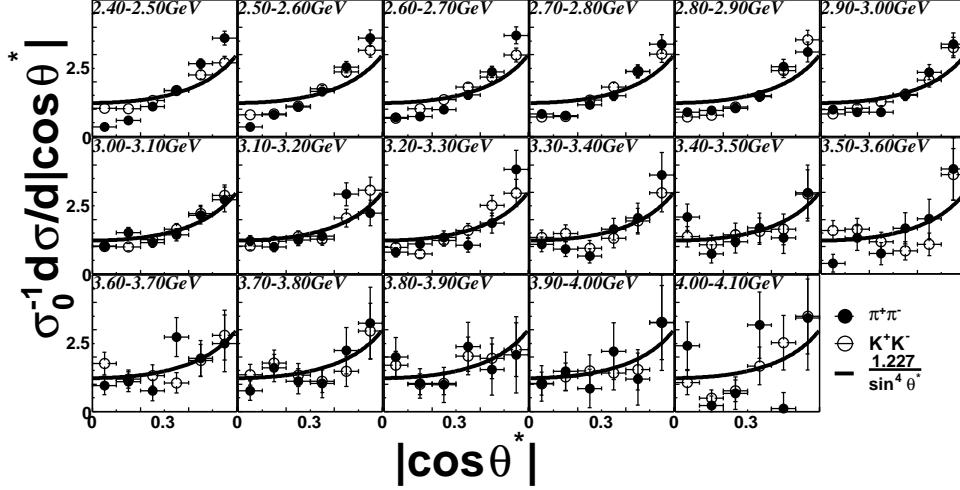


Fig. 4. Angular dependence of the cross section, $\sigma_0^{-1}d\sigma/d|\cos\theta^*|$, for the $\pi^+\pi^-$ (closed circles) and K^+K^- (open circles) processes. The curves are $1.227 \times \sin^{-4}\theta^*$. The errors are statistical only.

$$\frac{d\sigma}{d|\cos\theta^*|}(W, |\cos\theta^*|; \gamma\gamma \rightarrow X) = \frac{\Delta N(W, |\cos\theta^*|; e^+e^- \rightarrow e^+e^-X)}{L_{\gamma\gamma}(W)\Delta W\Delta|\cos\theta^*|\epsilon(W, |\cos\theta^*|)f\mathcal{L}dt} \quad (2)$$

where N and ϵ denote the number of the signal events and a product of detection and trigger efficiencies, respectively; $f\mathcal{L}dt$ is the integrated luminosity, and $L_{\gamma\gamma}$ is the luminosity function, defined as $L_{\gamma\gamma}(W) = \frac{d\sigma}{dW}(W; e^+e^- \rightarrow e^+e^-X)/\sigma(W; \gamma\gamma \rightarrow X)$.

The efficiencies $\epsilon(W, |\cos\theta^*|)$ for $\gamma\gamma \rightarrow \pi^+\pi^-$ and $\gamma\gamma \rightarrow K^+K^-$ are obtained from a full Monte Carlo simulation [11], using the TREPS [12] program for the event generation as well as the luminosity function determination. The trigger efficiency is determined from the trigger simulator. The typical value of the trigger efficiency is $\sim 93\%$ for events in the acceptance.

The efficiency-corrected measured differential cross sections for $\gamma\gamma \rightarrow \pi^+\pi^-$ and $\gamma\gamma \rightarrow K^+K^-$, normalized to the partial cross section σ_0 for $|\cos\theta^*| < 0.6$, are shown in Fig. 4 for each 100 MeV wide W bin. The partial cross sections σ_0 for both processes, integrated over the above scattering angle range, are shown in Fig. 5 (along with their ratio) and itemized in Table 1.

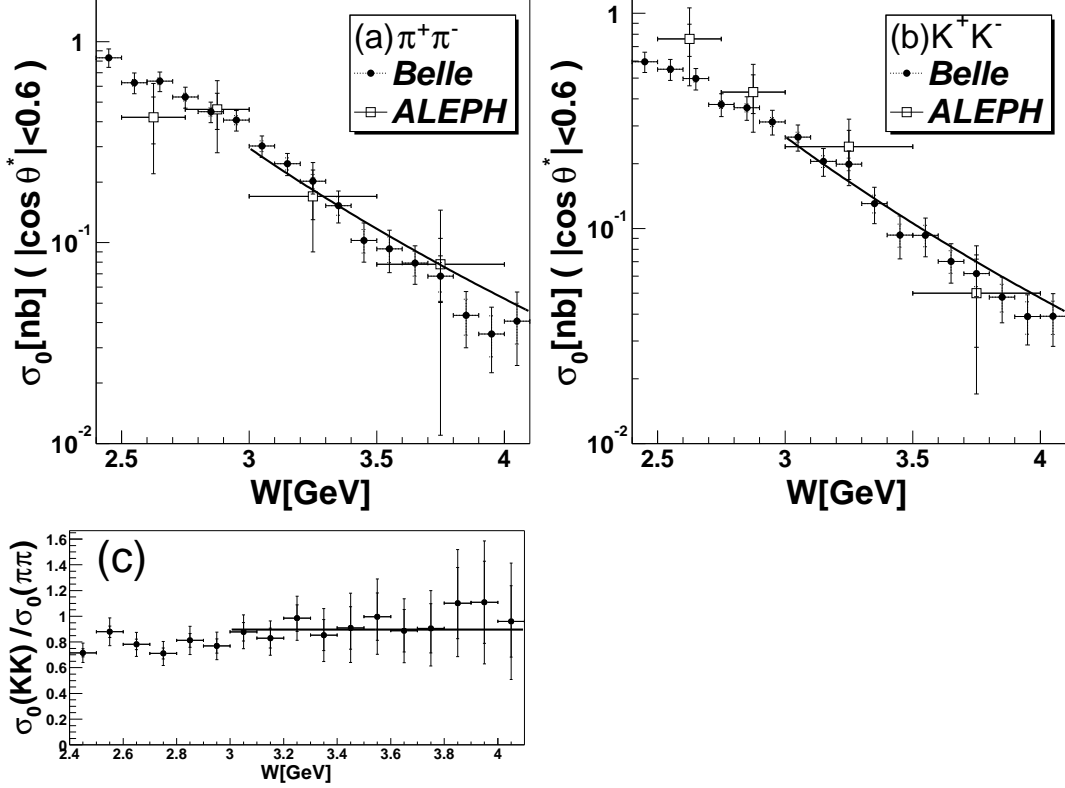


Fig. 5. Cross section for (a) $\gamma\gamma \rightarrow \pi^+\pi^-$, (b) $\gamma\gamma \rightarrow K^+K^-$ in the c.m. angular region $|\cos\theta^*| < 0.6$ together with a W^{-6} dependence line derived from the fit of $s|R_M|$. (c) shows the cross section ratio. The solid line is the result of the fit for the data above 3 GeV. The errors indicated by short ticks are statistical only.

6 Systematic errors

The dominant systematic errors are listed in Table 2. The uncertainty due to trigger efficiency is estimated by comparing the yields of $\gamma\gamma \rightarrow \mu^+\mu^-$ in real and simulated data [9] after accounting for the background from $e^+e^- \rightarrow \mu^+\mu^- n\gamma$ events (varying with W from 0.5–4.6%), which have the same topology [13]. The uncertainty in the relative muon identification efficiency between real and simulated data is used to determine the error associated with the residual $\mu^+\mu^-$ subtraction from the $\pi^+\pi^-$ sample. We use an error of 100% of the subtracted value for the non-exclusive background subtraction. We allow the number of χ_{cJ} events to fluctuate by up to 20% of the measured excess to estimate the error due to the χ_c subtraction that is applied for the energy bins in the range $3.3 \text{ GeV} < W < 3.6 \text{ GeV}$. The total W -dependent systematic error is 10–33% (10–21%) for the $\gamma\gamma \rightarrow \pi^+\pi^-$ ($\gamma\gamma \rightarrow K^+K^-$) cross section.

Table 1

Cross sections and errors for the $\gamma\gamma \rightarrow \pi^+\pi^-$ and $\gamma\gamma \rightarrow K^+K^-$ processes, in the angular range $|\cos \theta^*| < 0.6$.

W GeV	$\gamma\gamma \rightarrow \pi^+\pi^-$			$\gamma\gamma \rightarrow K^+K^-$		
	σ_0 nb	stat.err nb	syst.err nb	σ_0 nb	stat.err nb	syst.err nb
2.4-2.5	0.832	0.026	0.083	0.595	0.019	0.062
2.5-2.6	0.625	0.024	0.070	0.549	0.018	0.059
2.6-2.7	0.636	0.025	0.067	0.497	0.018	0.054
2.7-2.8	0.530	0.023	0.059	0.377	0.016	0.043
2.8-2.9	0.448	0.022	0.048	0.364	0.016	0.043
2.9-3.0	0.407	0.021	0.042	0.313	0.015	0.038
3.0-3.1	0.302	0.019	0.032	0.266	0.014	0.034
3.1-3.2	0.247	0.017	0.026	0.205	0.013	0.027
3.2-3.3	0.202	0.016	0.022	0.199	0.013	0.027
3.3-3.4	0.153	0.016	0.023	0.130	0.012	0.022
3.4-3.5	0.103	0.014	0.018	0.093	0.011	0.018
3.5-3.6	0.093	0.014	0.017	0.093	0.011	0.016
3.6-3.7	0.079	0.011	0.013	0.070	0.009	0.012
3.7-3.8	0.068	0.011	0.014	0.062	0.008	0.011
3.8-3.9	0.043	0.009	0.010	0.048	0.007	0.009
3.9-4.0	0.035	0.008	0.010	0.039	0.007	0.008
4.0-4.1	0.041	0.009	0.013	0.039	0.007	0.008

7 Discussion

For $\gamma\gamma \rightarrow \pi^+\pi^-$ and $\gamma\gamma \rightarrow K^+K^-$, Brodsky and Lepage predicted a $\sin^{-4} \theta^*$ dependence of the differential cross section [1] as seen in Eq. 1, and Brodsky and Farrar (BF) predicted a W^{-6} dependence of the cross section [14]. The soft hadron exchange (“handbag”) model by DKV [4] predicts an expression for the differential cross section similar to Eq. 1

$$\frac{d\sigma}{d|\cos \theta^*|}(\gamma\gamma \rightarrow M^+M^-) \approx \frac{8\pi\alpha^2}{s} \frac{|R_{2M}(s)|^2}{\sin^4 \theta^*}, \quad (3)$$

Table 2

Contributions to the systematic errors. A range is shown when the error has a W dependence.

Source	$\pi^+\pi^-$	K^+K^-
Tracking efficiency	4%	4%
Trigger efficiency	4%	4%
K/π separation	0–1%	2–4%
$\mu\mu$ background subtraction	5–17%	0%
Non-exclusive background subtraction	4–27%	7–20%
Luminosity function	5%	5%
Integrated luminosity	1%	1%
χ_c subtraction ($3.3 \text{ GeV} < W < 3.6 \text{ GeV}$)	8–11%	8–11%
Total	10–33%	10–21%

where M denotes either a pion or a kaon. Here, they introduce the “annihilation form factor” $R_{2M}(s)$, which can be determined experimentally.

Fig. 4 shows normalized angular distributions as a function of W , for $\pi^+\pi^-$ and K^+K^- modes. The solid curves indicate the expectations from a $\sin^{-4}\theta^*$ behavior predicted by BL and DKV models

$$\frac{1}{\sigma_0} \frac{d\sigma}{d|\cos\theta^*|} = \frac{1.227}{\sin^4\theta^*}. \quad (4)$$

These curves match the data well for $3.0 \text{ GeV} < W < 4.1 \text{ GeV}$, but are more shallow than the data for $W < 3.0 \text{ GeV}$. This disagreement may arise from the presence of one or more lower-energy resonances: for example, Belle has reported a resonance at $(2327 \pm 6 \pm 6) \text{ MeV}/c^2$ with a width of $(275 \pm 12 \pm 20) \text{ MeV}/c^2$ in a study of $\gamma\gamma \rightarrow K^+K^-$ with $W < 2.4 \text{ GeV}$ [15]. Small momentum transfer from the photons to the pions, $-t < 3 \text{ GeV}^2$ at smaller scattering angles, may also cause this disagreement for $W < 3.0 \text{ GeV}$ through some unknown non-perturbative or hadronic effects.

We extract the annihilation form factor $R_{2M}(s)$ directly from the data, by integrating the observed cross sections over $|\cos\theta^*| < 0.6$ in the range of $3.0 \text{ GeV} < W < 4.1 \text{ GeV}$, where Eq. 4 fits the data quite well. Since the observed values of $s|R_{2M}(s)|$ are almost W -independent, we obtain $s|R_{2\pi}| = 0.71 \pm 0.01 \pm 0.05 \text{ GeV}^2$ and $s|R_{2K}| = 0.68 \pm 0.01 \pm 0.05 \text{ GeV}^2$ by fits to the data in this W range. Fig. 5 shows the observed cross sections in comparison with the recent ALEPH data [5]. The lines indicate expectations with the $s|R_{2M}(s)|$

values from the fit above. Our data are consistent with W^{-6} behavior predicted by BL [1] and BF [14] models.

We can also directly obtain the power n of the W -dependence ($\sigma_0 \propto W^n$) from the data. We find $n = -7.9 \pm 0.4 \pm 1.5$ for $\pi^+\pi^-$ and $-7.3 \pm 0.3 \pm 1.5$ for K^+K^- , for $3.0 \text{ GeV} < W < 4.1 \text{ GeV}$. The first error is statistical, and the second is systematic. We conservatively estimate the systematic error of n by artificially deforming the measured cross section values under the assumption that systematic errors are strongly point-to-point correlated: we shift the σ_0 values at the two end bins by ± 1.5 and ∓ 1.5 times the systematic error, respectively, whereas each intermediate point is correspondingly moved so that its shift follows a linear function of W times its systematic error. The average of the observed deviations of n from its original value is taken as a final systematic error. The results show a hint of somewhat steeper dependence than W^{-6} .

Fig. 5(c) shows the cross section ratio $\sigma_0(\gamma\gamma \rightarrow K^+K^-)/\sigma_0(\gamma\gamma \rightarrow \pi^+\pi^-)$ as a function of W . The ratio is energy independent for $3.0 \text{ GeV} < W < 4.1 \text{ GeV}$, in accordance with the QCD prediction. The obtained value of the ratio is $0.89 \pm 0.04(\text{stat.}) \pm 0.15(\text{syst.})$. It is consistent with the value of 1.08 predicted by Benayoun and Chernyak (BC) [16] and significantly below 2.23 following from the BL calculation [1] and using the current values of the kaon and pion decay constants [17]. The value predicted by BC is a consequence of consistent consideration of the SU(3) breaking effects using the different wave functions for pions and kaons derived from the QCD sum rules. This compensates for the partial account of the SU(3) breaking by BL who used the same wave functions for pions and kaons so that the cross section ratio is equal to the fourth power of the ratio of the kaon and pion decay constants.

8 TWO-PHOTON DECAY WIDTH OF χ_{cJ} RESONANCES

The measured yields of χ_{c0} and χ_{c2} events can be used to extract the two-photon decay width of each resonance using the formula

$$\Gamma_{\gamma\gamma}(\chi_{cJ}) = \frac{Y M_{cJ}^2}{4(2J+1)\pi^2 L_{\gamma\gamma}(M_{cJ}) \epsilon \mathcal{B}(\chi_{cJ} \rightarrow M^+ M^-) \int \mathcal{L} dt} \quad (5)$$

where Y and M_{cJ} are the yield and mass, respectively, of the corresponding spin- J χ_{cJ} resonance (where the mass is taken from Ref. [17]). ϵ denotes the product of the detection efficiency and acceptance for the resonance decays. The extracted values of $\Gamma_{\gamma\gamma}(\chi_{cJ}) \mathcal{B}(\chi_{cJ} \rightarrow M^+ M^-)$ are summarized in Table 3. The ratios $\Gamma_{\gamma\gamma} \mathcal{B}(K^+K^-)/\Gamma_{\gamma\gamma} \mathcal{B}(\pi^+\pi^-)$ are consistent with the known $\mathcal{B}(K^+K^-)/\mathcal{B}(\pi^+\pi^-)$ [17] ratios for both resonances. Therefore

Table 3

Results for the product of the two-photon decay width and the branching fraction, $\Gamma_{\gamma\gamma}(\chi_{cJ})\mathcal{B}(\chi_{cJ} \rightarrow M^+M^-)$. The second column gives the observed χ_{cJ} yields in the W region of 3.34–3.44 GeV (3.54–3.58 GeV) for χ_{c0} (χ_{c2}). The first and second errors for $\Gamma_{\gamma\gamma}\mathcal{B}$ are statistical and systematic, respectively.

	Number of events	$\Gamma_{\gamma\gamma}(\chi_{cJ})\mathcal{B}(\chi_{cJ} \rightarrow M^+M^-)[\text{eV}]$	Significance
$\gamma\gamma \rightarrow \chi_{c0} \rightarrow \pi^+\pi^-$	129 ± 18	$15.1 \pm 2.1 \pm 2.6$	6.2σ
$\gamma\gamma \rightarrow \chi_{c0} \rightarrow K^+K^-$	153 ± 17	$14.3 \pm 1.6 \pm 2.7$	8.2σ
$\gamma\gamma \rightarrow \chi_{c2} \rightarrow \pi^+\pi^-$	54 ± 10	$0.76 \pm 0.14 \pm 0.14$	4.8σ
$\gamma\gamma \rightarrow \chi_{c2} \rightarrow K^+K^-$	33 ± 8	$0.44 \pm 0.11 \pm 0.07$	3.7σ

we combine the measurements of the widths from the two modes to obtain $\Gamma_{\gamma\gamma}(\chi_{c0}) = 2.62 \pm 0.23(\text{stat.}) \pm 0.50(\text{syst.}) \pm 0.28(\mathcal{B})$ keV and $\Gamma_{\gamma\gamma}(\chi_{c2}) = 0.44 \pm 0.07(\text{stat.}) \pm 0.09(\text{syst.}) \pm 0.06(\mathcal{B})$ keV where the error associated with the branching fraction (taken from [17]) is calculated assuming independent uncertainties for the $\pi^+\pi^-$ and K^+K^- modes. These values are consistent with the two-photon decay widths of χ_{c0} and χ_{c2} following from the total widths and branching ratios into two photons obtained in previous experiments [17].

9 Conclusion

Using 87.7 fb^{-1} of data collected with the Belle detector at KEKB, we have measured with high precision the cross sections for the $\gamma\gamma \rightarrow \pi^+\pi^-$ and $\gamma\gamma \rightarrow K^+K^-$ processes in the two-photon c.m. energy range $2.4 \text{ GeV} < W < 4.1 \text{ GeV}$ and angular range of $|\cos\theta^*| < 0.6$.

The angular differential cross sections for those processes show a $\sin^{-4}\theta^*$ behavior in the range of $3.0 \text{ GeV} < W < 4.1 \text{ GeV}$, which is predicted by QCD. The energy dependence of the differential cross section is also consistent with the QCD prediction of $\sigma \propto W^{-6}$. The partial cross section ratio $\sigma_0(\gamma\gamma \rightarrow K^+K^-)/\sigma_0(\gamma\gamma \rightarrow \pi^+\pi^-)$, in $|\cos\theta^*| < 0.6$ is measured to be $0.89 \pm 0.04(\text{stat.}) \pm 0.15(\text{syst.})$ for $3.0 \text{ GeV} < W < 4.1 \text{ GeV}$ in accordance with the prediction based on the QCD sum rules and SU(3) symmetry breaking.

We have observed the χ_{c0} and χ_{c2} resonances decaying to $\pi^+\pi^-$ and K^+K^- final states and measured the products of their two-photon decay widths and two-hadron branching fractions for the first time.

Acknowledgements

We thank the KEKB group for the excellent operation of the accelerator, the KEK Cryogenics group for the efficient operation of the solenoid, and the KEK computer group and the National Institute of Informatics for valuable computing and Super-SINET network support. We are grateful to V. Chernyak for fruitful discussions. We acknowledge support from the Ministry of Education, Culture, Sports, Science, and Technology of Japan and the Japan Society for the Promotion of Science; the Australian Research Council and the Australian Department of Education, Science and Training; the National Science Foundation of China under contract No. 10175071; the Department of Science and Technology of India; the BK21 program of the Ministry of Education of Korea and the CHEP SRC program of the Korea Science and Engineering Foundation; the Polish State Committee for Scientific Research under contract No. 2P03B 01324; the Ministry of Science and Technology of the Russian Federation; the Ministry of Education, Science and Sport of the Republic of Slovenia; the Swiss National Science Foundation; the National Science Council and the Ministry of Education of Taiwan; and the U.S. Department of Energy.

References

- [1] S. J. Brodsky and G. P. Lepage, *Phys. Rev. D* **24** (1981) 1808.
- [2] C. Vogt, in Proceedings of PHOTON 2000: Ambleside, England, August 26th-31st, American Institute of Physics (2001), 345.
- [3] J. Dominick *et al.*, CLEO Collaboration, *Phys. Rev. D* **50** (1994) 3027.
- [4] M. Diehl, P. Kroll and C. Vogt, *Phys. Lett. B* **532** (2002) 99.
- [5] A. Heister *et al.*, ALEPH Collaboration, *Phys. Lett. B* **569** (2003) 140.
- [6] A. Abashian *et al.*, Belle Collaboration, *Nucl. Instr. Meth. A* **479** (2002) 117.
- [7] S. Kurokawa and E. Kikutani, *Nucl. Instr. Meth. A* **499** (2003) 1.
- [8] S. Jadach and Z. Wąs, *Comp. Phys. Commun.* **85** (1995) 453.
- [9] F. A. Berends, P. H. Daverveldt and R. Kleiss, *Nucl. Phys. B* **253** (1985) 441;
F. A. Berends, P. H. Daverveldt and R. Kleiss, *Comp. Phys. Commun.* **40** (1986) 285.
- [10] K. Abe *et al.*, *Phys. Lett. B* **540** (2002) 33.
- [11] The detector response is simulated with GEANT, R. Brun *et al.*, GEANT 3.21, CERN Report DD/EE/84-1, 1984.
- [12] S. Uehara, KEK Report 96-11 (1996).

- [13] S. Jadach, B. F. L. Ward and Z. Wąs, *Comp. Phys. Commun.* **130** (2000) 260.
- [14] S. J. Brodsky and G. R. Farrar, *Phys. Rev. D* **11** (1975) 1309.
- [15] K. Abe *et al.*, Belle Collaboration, *Eur. Phys. J. C* **32** (2003) 323.
- [16] M. Benayoun and V. L. Chernyak, *Nucl. Phys. B* **329** (1990) 285.
- [17] S. Eidelman *et al.*, *Phys. Lett. B* **592** (2004) 1.